AMERICAN SOCIETY FOR MICROBIOLOGY | Applied and Environmental Microbiology®

BIOTECHNOLOGY

Reexamination of the Physiological Role of PykA in *Escherichia coli* Revealed that It Negatively Regulates the Intracellular ATP Levels under Anaerobic Conditions

Chunhua Zhao,[a,b] Zhao Lin,[a,b] Hongjun Dong,[a] Yanping Zhang,[a] Yin Li[a]

CAS Key Laboratory of Microbial Physiological and Metabolic Engineering, Institute of Microbiology, Chinese Academy of Sciences, Beijing, China[a]; University of Chinese Academy of Sciences, Beijing, China[b]

ABSTRACT Pyruvate kinase is one of the three rate-limiting glycolytic enzymes that catalyze the last step of glycolysis, conversion of phosphoenolpyruvate (PEP) into pyruvate, which is associated with ATP generation. Two isozymes of pyruvate kinase, PykF and PykA, are identified in *Escherichia coli*. PykF is considered important, whereas PykA has a less-defined role. Prior studies inactivated the *pykA* gene to increase the level of its substrate, PEP, and thereby increased the yield of end products derived from PEP. We were surprised when we found a *pykA*::Tn*5* mutant in a screen for increased yield of an end product derived from pyruvate (*n*-butanol), suggesting that the role of PykA needs to be reexamined. We show that the *pykA* mutant exhibited elevated intracellular ATP levels, biomass concentrations, glucose consumption, and *n*-butanol production. We also discovered that the *pykA* mutant expresses higher levels of a presumed pyruvate transporter, YhjX, permitting the mutant to recapture and metabolize excreted pyruvate. Furthermore, we demonstrated that the nucleotide diphosphate kinase activity of PykA leads to negative regulation of the intracellular ATP levels. Taking the data together, we propose that inactivation of *pykA* can be considered a general strategy to enhance the production of pyruvate-derived metabolites under anaerobic conditions.

IMPORTANCE This study showed that knocking out *pykA* significantly increased the intracellular ATP level and thus significantly increased the levels of glucose consumption, biomass formation, and pyruvate-derived product formation under anaerobic conditions. *pykA* was considered to be encoding a dispensable pyruvate kinase; here we show that *pykA* negatively regulates the anaerobic glycolysis rate through regulating the energy distribution. Thus, knocking out *pykA* can be used as a general strategy to increase the level of pyruvate-derived fermentative products.

KEYWORDS ATP, anaerobic condition, *Escherichia coli*, physiological role, PykA

Received 5 February 2017 **Accepted** 24 March 2017

Accepted manuscript posted online 31 March 2017

Citation Zhao C, Lin Z, Dong H, Zhang Y, Li Y. 2017. Reexamination of the physiological role of PykA in *Escherichia coli* revealed that it negatively regulates the intracellular ATP levels under anaerobic conditions. Appl Environ Microbiol 83:e00316-17. https://doi.org/10.1128/AEM.00316-17.

Editor Rebecca E. Parales, University of California, Davis

Address correspondence to Hongjun Dong, redarmy305@gmail.com, or Yin Li, yli@im.ac.cn.

Industrial fermentation aims to produce valuable products from cheap feedstocks by utilizing the diverse functions of microbes. Products such as antibiotics, amino acids, and vitamins are mostly produced through aerobic fermentations, while products such as alcohols (ethanol, butanol, butanediol) are mainly produced through anaerobic fermentation (1–3). Organic acids such as lactic acid and succinic acid are also produced through anaerobic fermentation because higher yields could be obtained (4, 5).

During anaerobic fermentation, the reducing power is directed mostly to producing synthesis rather than to oxidization, resulting in a higher yield of target products. In addition, the low energy level due to the absence of oxidative phosphorylation often leads to a higher glycolysis rate, resulting in higher productivity (6). However, as the available ATP in anaerobic fermentation can be generated only from substrate-level phosphorylation, the biomass concentration in anaerobic fermentation is usually much

TABLE 1 The *n*-butanol production of the basic strains[a]

Strain	Glucose consumed (g/liter)	*n*-Butanol produced (g/liter)	% yield (g/g)
EB205	4.83 ± 0.22	0.47 ± 0.03	9.7
EB215	13.45 ± 0.04	0.87 ± 0.03	13.2
EB216	11.12 ± 0.18	1.60 ± 0.12	18.0

[a]The strains were grown in static 15-ml sealed BD tubes for determination of *n*-butanol production at 37°C for 72 h. Three repeats were performed, and the error data represent standard deviations.

lower than that in aerobic fermentation (2, 7). Although a lower energy charge in anaerobic fermentation is beneficial for increasing the glycolysis rate (8–10), it has been shown that increasing the ATP concentration can improve protein synthesis and increase biomass flux during anaerobic fermentation (11, 12). This suggests that factors affecting the intracellular ATP level may well be the targets for engineering to increase the efficiency of anaerobic fermentation processes.

There are three rate-limiting enzymes in glycolysis, i.e., hexokinase, phosphofructokinase, and pyruvate kinase, among which only pyruvate kinase is associated with ATP generation (13). Pyruvate kinase catalyzes the last step of glycolysis, converting phosphoenolpyruvate (PEP) into pyruvate. This step can also be catalyzed by the glucose-specific transporter PtsG of the phosphotransferase system, but no free ATP would be generated (14). In *Escherichia coli*, there are two pyruvate kinase isoenzymes, PykF and PykA, encoded by the *pykF* and *pykA* genes, respectively. PykF is characterized as an enzyme that is allosterically activated by fructose-1,6-bisphosphatase (FBP), whereas PykA is activated by AMP (15). In activity assays, the activity of PykF significantly surpasses that of PykA under aerobic conditions in the same reaction system using purified enzymes or crude extracts (15–17). It is generally believed that PykF contributes to a greater extent to the activity of pyruvate kinase, while PykA contributes little (18).

However, in our previous study, inactivation of *pykA* in an engineered *n*-butanol-producing *E. coli* strain was found to increase the glucose consumption rate and the *n*-butanol production rate under anaerobic conditions (17). This surprising observation suggests that the physiological roles of PykA in glycolysis have been overlooked and should be reexamined. We therefore designed a series of experiments to better understand the physiological role of PykA in anaerobic fermentation.

RESULTS

Construction of the basic *n*-butanol-producing *E. coli* strain. Genes involved in the *n*-butanol synthetic pathway (*atoB*, *hbd*, *crt*, *ter*, *adhE2*, and *fdh*) were chosen according to the published research (2, 19). For construction of a genetically stable strain for *n*-butanol production that may have industrial application potential, we managed to integrate these genes into the chromosome of *E. coli*, which is different from all previous reported work. Six genes under the control of the miniPtac promoter (20) were successfully integrated into wild-type BW25113 to generate strain EB205, while genes involved in pathways for production of native fermentative by-products (ethanol, lactate, acetate, and succinate) were disrupted simultaneously. In order to remove the native formate lysis pathway and improve the NADH supply, the *hyc* operon and *hyp* operon were deleted and a codon-optimized *fdh* gene (the specific sequence is available in the supplemental material) was introduced in strain EB205, resulting in strain EB215. Further, the *mdh* gene involved in fumarate pathway competition for NADH was deleted to generate strain EB216. Thus, *n*-butanol-producing strain EB216, with all heterologously introduced genes integrated into the chromosome, was successfully constructed and used as a starting strain for this study. Tube fermentation results determined for strains EB205, EB215, and EB216 are shown in Table 1.

Finding new targets for improving *n*-butanol production using Tn*5* transposon mutation. A Tn*5* transposon was introduced into strain EB216 with the aim to discover new gene targets that may contribute to improved *n*-butanol producers. A total of

TABLE 2 The effect of *pykA* inactivation on utilization of glucose for *n*-butanol production[a]

Strain	OD_{600}	Glucose consumed (g/liter)	Level of product (g/liter)		% yield (g/g)
			Pyruvate	*n*-Butanol	
EB216	1.44 ± 0.02	8.09 ± 0.40	1.28 ± 0.04	1.38 ± 0.16	17
EB216-Tn5-599#	1.83 ± 0.04	10.88 ± 0.21	0.59 ± 0.07	2.52 ± 0.18	23
EB216-ΔpykA	1.74 ± 0.02	10.49 ± 0.15	0.43 ± 0.09	2.37 ± 0.10	23

[a]The strains were grown in static 15-ml sealed BD tubes for determination of *n*-butanol production at 37°C for 48 h. EB216 is the control strain. The *pykA* gene was inactivated by insertion of a Tn*5* transposon in strain EB216-Tn5-599# or by deletion in strain EB216-ΔpykA. Three repeats were performed, and the error data represent standard deviations.

1,196 mutants were screened in the first round; among those, 200 mutants that performed well were selected for the second round, high-performance liquid chromatography (HPLC) screening, and 16 mutants were obtained. After repeated tube fermentations, 3 mutants among 16 screened in the second-round screening showed significantly increased *n*-butanol production. The *n*-butanol titers of mutants EB216-Tn5-17#, EB216-Tn5-304#, and EB216-Tn5-599# increased 29%, 49%, and 57%, respectively (data not shown) (17). Strain EB216-Tn5-599# was the most interesting mutant, as next-generation sequencing (NGS) indicated that the Tn*5* transposon had inserted into *pykA*, a gene which is involved in glycolysis (17).

Inactivation of the *pykA* gene improved utilization of glucose and *n*-butanol production. Strain EB216-Tn5-599# described above produced 2.5 g/liter *n*-butanol, which is 1.8-fold the level produced by strain EB216 in tube fermentations (Table 2). To exclude any potential bias represented by the introduced Tn*5* transposon, the *pykA* open reading frame in strain EB216 was deleted, generating strain EB216-ΔpykA (also named as EB222). Table 2 shows that strain EB216-Tn5-599# and strain EB216-ΔpykA exhibited similar abilities with respect to glucose consumption and *n*-butanol production ($P > 0.05$), which increased by over 30% and 70%, respectively, compared with the results seen with strain EB216. This suggests that the *pykA* clean deletion mutant behaves similarly to the Tn*5* insertion mutant, demonstrating that inactivation of *pykA* indeed improved glucose consumption and *n*-butanol production.

Fermentation performance of the *pykA*-inactivated mutant. To better understand the effect of *pykA* inactivation on cellular metabolism, fermentation profiles of strain EB216 and strain EB216-ΔpykA were monitored. As shown in Fig. 1, cell growth (Fig. 1A), glucose consumption (Fig. 1B), and *n*-butanol production (Fig. 1C) of strain EB216-ΔpykA all significantly improved compared with that of the control strain. In addition, acetate and butyrate titers also increased as more glucose was consumed in strain EB216-ΔpykA. Among the profiles of other metabolites, the most significant difference exists in the production of pyruvate. Strain EB216 produced 1.36 g/liter pyruvate at 12 h, and the pyruvate concentration did not change significantly afterwards. Strain EB216-ΔpykA, however, produced only 0.71 g/liter of pyruvate at 12 h, followed by a decline of the pyruvate concentration, suggesting reassimilation (Fig. 1I). Glucose distribution analysis showed that the significantly increased (Table 3, bold) glucose-to-butanol ratio (68%) in strain EB216-ΔpykA can be ascribed to the significantly decreased (Table 3, italics) glucose-to-pyruvate ratio (3%).

The *yhjX* gene is involved in pyruvate reassimilation. One of the important characteristics of the EB216-ΔpykA strain is its reutilization of the secreted pyruvate. Interestingly, from examination of the transcriptomic analysis data (see Table S1 in the supplemental material), we found that the *yhjX* gene, which encodes a putative pyruvate transporter (22–24), was 15-fold upregulated compared with the control strain EB216 at 48 h. Figure 2A shows that the expression strength of the *yhjX* gene is highly associated with the fermentation process (from 216 to 5,703 fragments per kilobase per million reads [FPKM], which was 10 to 15 times higher than that measured in strain EB216 during the *n*-butanol-producing period). To investigate whether *yhjX* is associated with pyruvate reassimilation, the *yhjX* gene was knocked out in the EB216 and

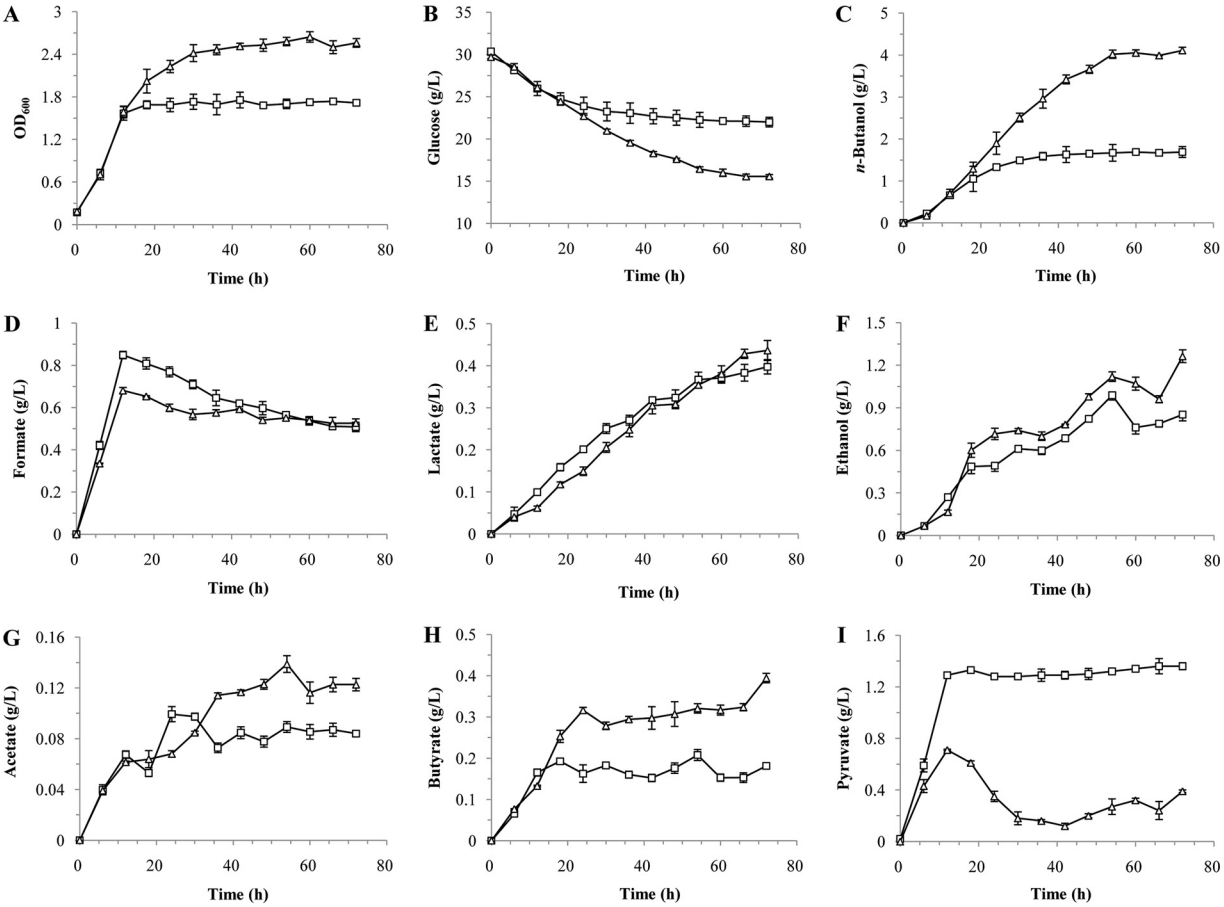

FIG 1 Fermentation profiles of strain EB216 (squares) and strain EB216-ΔpykA (triangles). Fermentation was performed in 7.5-liter bioreactors with an initial working volume of 4 liters. Data shown represent averages of results from three independent batch cultures, and the error bars represent standard deviations. (A) Cell growth. (B) Glucose. (C) *n*-Butanol. (D) Formate. (E) Lactate. (F) Ethanol. (G) Acetate. (H) Butyrate. (I) Pyruvate.

EB216-ΔpykA strains. The results showed that the two *yhjX* mutant strains produced more pyruvate and less *n*-butanol (Fig. 2B). Hence, *yhjX* is an important target for further metabolic engineering.

Reexamination and comparison of the roles of *pykA* and *pykF*. Fermentation and transcriptomic analyses showed that strain EB216-ΔpykA is the more active and robust strain (Fig. 1; see also Fig. S1 and Table S1 in the supplemental material). To further understand the role of *pykA* and the corresponding *pykF* isoenzyme gene under the circumstance of *n*-butanol production, we constructed a *pykF* mutant strain, the EB216-ΔpykF mutant. Strain EB216-ΔpykA and the EB216-ΔpykF mutant were subjected

TABLE 3 Comparison of end product titers and glucose distribution between strain EB216 and EB216-ΔpykA

Strain	Titer (in mM) of end product (%)[a]							
	Biomass[b]	Pyruvate	Lactate	Acetate	Ethanol	Butyrate	*n*-Butanol	Gluc. cons.[c]
EB216	*15.42 (6)*	*15.45 (16)*	*8.64 (9)*	1.38 (1)	*18.53 (20)*	**2.06 (4)**	**22.84 (49)**	46.39 (107[d])
EB216-ΔpykA	*23.83 (5)*	*4.43 (3)*	*9.49 (6)*	2.01 (1)	*27.46 (17)*	**4.48 (5)**	**55.54 (68)**	78.50 (109[d])

[a]Calculations were performed on the basis of the data collected at the final point (72 h) as indicated in Fig. 1. Each value indicates the glucose distribution for specific end product, which is the value of the theoretical amount of glucose consumed for one end product divided by the practical amount of total consumed glucose. Italic highlighting indicates decreased glucose distribution. Bold highlighting indicates increased glucose distribution.

[b]The biomass was calculated from the OD_{600} using the following equation: biomass (in grams per liter) = $OD_{600} \times 0.25$. The molecular formula for *E. coli* biomass is $CH_{1.77}O_{0.49}N_{0.24}$ (21).

[c]Gluc. cons., total glucose consumed in 72 h.

[d]The value indicates the carbon balance, which is calculated as the amount of glucose theoretically used for all the detected end products divided by the amount of glucose used in practice. The total value exceeds 100% due to the presence of yeast extract.

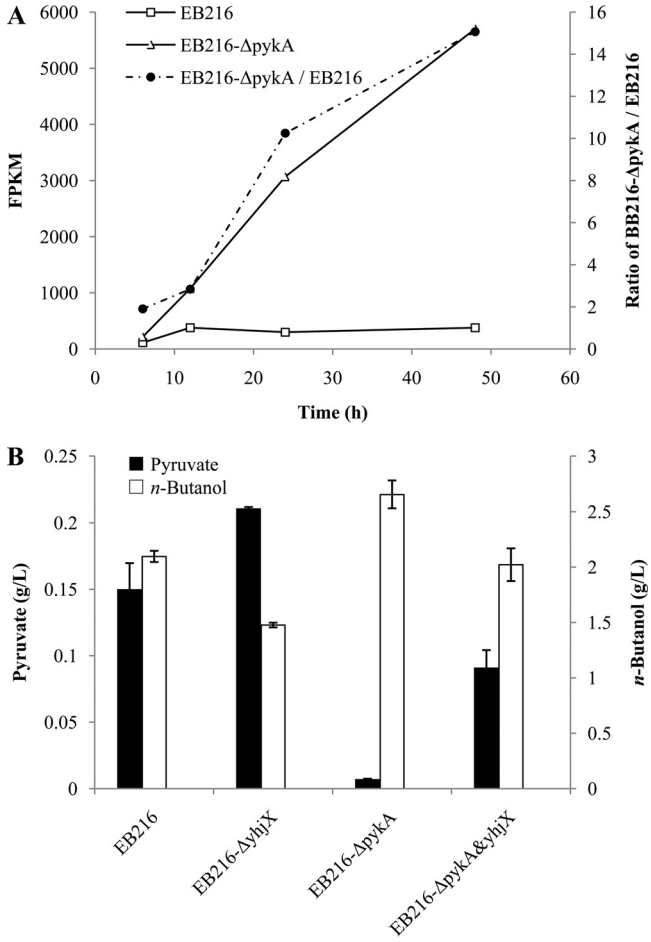

FIG 2 The role of *yhjX* gene in fermentative production of *n*-butanol. Three repeats were performed, and the error bars represent standard deviations. (A) The expression strength of *yhjX* gene in strain EB216 and strain EB216-ΔpykA. The expression strength is shown as the values of FPKM calculated using the RSEM software tool (V 1.2.4). (B) The pyruvate and *n*-butanol production of *yhjX*-deleted strains derived from strain EB216 and strain EB216-ΔpykA. The strains were grown in static 15-ml sealed BD tubes for *n*-butanol production at 37°C for 48 h.

to a series of biochemical analyses, with the aim to gain more insights into the physiological role of PykA and PykF in an *n*-butanol-producing strain.

Pyruvate kinase assays of the *E. coli* EB216 strain (Table 4) showed that the activity of PykF accounted for 93% of the total pyruvate kinase activity, while that of PykA accounted for only 7%, under aerobic conditions. This is consistent with the previous recognition that PykF is the main pyruvate kinase in *E. coli* (25, 26). However, under anaerobic conditions, the activity of PykF accounted for 70% of the total pyruvate

TABLE 4 Assay of pyruvate kinase activity[a]

	Culture result (U/mg)			
	Anaerobic		Aerobic	
Strain	PykF	PykA	PykF	PykA
EB216	0.72 ± 0.09	0.31 ± 0.03	0.57 ± 0.04	0.04 ± 0.00
EB216-ΔpykF	ND	0.35 ± 0.05	ND	0.05 ± 0.00
EB216-ΔpykA	0.76 ± 0.09	ND	0.50 ± 0.03	ND

[a]U, 1 unit of pyruvate kinase generates 1 μmol pyruvate and 1 μmol ATP from PEP and ADP per minute under the test conditions (25°C, pH 7.5). mg, milligrams of crude protein extract. ND, not detectable. For anaerobic culture, the strains were grown in static 15-ml sealed BD tubes at 37°C; for aerobic culture, the strains were grown in 50-ml half-sealed BD tubes in a 220-rpm shaker at 37°C. The working volume was 10 ml in both experiments. Three repeats were performed, and the error data represent standard deviations.

TABLE 5 Kinetic parameters of purified His-tagged PykA and PykF[a]

Substrate	PykA			PykF		
	K_m (mM)	k_{cat} (s^{-1})	k_{cat}/K_m (M^{-1} s^{-1})	K_m (mM)	k_{cat} (s^{-1})	k_{cat}/K_m (M^{-1} s^{-1})
ADP	0.060 ± 0.009	129 ± 14	(2.17 ± 0.26) × 10^6	0.210 ± 0.066	80 ± 11	(3.99 ± 0.80) × 10^5
UDP	0.089 ± 0.019	164 ± 20	(1.88 ± 0.22) × 10^6	0.648 ± 0.085	166 ± 29	(2.55 ± 0.19) × 10^5
GDP	0.345 ± 0.036	209 ± 17	(6.07 ± 0.20) × 10^5	ND	ND	ND
CDP	0.560 ± 0.028	43 ± 2	(7.71 ± 0.32) × 10^4	ND	ND	ND

[a]ND, not detectable. *E. coli* BL21(DE3) and pET30a vector were used to express the His-tagged pyruvate kinases. The *pykA* gene was amplified from genomic DNA of BW25113 with primers pykA-NdeI-1 and pykAChis-XhoI-2 (Table S2) and cloned into pET30a vector through NdeI and XhoI sites, while the *pykF* gene was amplified from genomic DNA of BW25113 with primers pykF-NdeI-1 and pykFChis-HindIII-2 (Table S2) and cloned into pET30a vector through NdeI and HindIII sites. The Michaelis-Menten equation was used to calculate the kinetic parameters. Three repeats were performed, and the error data represent standard deviations.

kinase activity, while that of PykA accounted for 30%. This indicates that PykA plays a more important role under anaerobic conditions than under aerobic conditions. Moreover, it was observed that knocking out *pykF* would not affect the absolute activity of PykA, and that knocking out *pykA* would not affect the absolute activity of PykF, under both aerobic and anaerobic conditions. This suggests that the activity of PykF and that of PykA are independent of those of their counterparts.

We also noticed that previous reports have indicated that PykA is capable of catalyzing four kinds of nucleoside diphosphate kinases (NDPs) (ADP, UDP, GDP, and CDP) to nucleoside triphosphates (NTPs) in the reaction of PEP to pyruvate, while PykF typically uses ADP as the substrate to form ATP (27–30). To study the selectivity of NDP with respect to PykF or PykA, we did the pyruvate kinase assay and determined the kinetic parameters by replacing ADP with UDP, GDP, or CDP using the purified enzymes. The specificity constants (k_{cat}/K_m) of PykA and PykF on four NDPs were determined. Results showed that PykA was broadly active on the four NDPs, while PykF was active only on ADP and UDP (Table 5). Strikingly, the k_{cat}/K_m of PykA on ADP and UDP is about 1 order of magnitude higher than that of PykF, while the k_{cat}/K_m of PykA on GDP is at the same magnitude but is still higher than that of PykF on ADP and UDP. CDP is the last substrate choice, according to the results. We therefore further analyzed the intracellular ATP concentrations of strains EB216, EB216-ΔpykF, and EB216-ΔpykA. The results showed that the intracellular ATP concentration of strain EB216-ΔpykA increased by 150% compared with strain EB216 (Table 6). This suggests that the phosphorus groups that were used for generation of GTP and CTP by PykA might have been redirected for generation of ATP and UTP by PykF, resulting in an increased intracellular concentration of ATP, and enabled strain EB216-ΔpykA grow to a higher cell density (Fig. 1A).

In addition, the NADH which is the reducing power for *n*-butanol formation was also measured. NADH assay showed that the intracellular NADH level of strain EB216-ΔpykF did not significantly differ from that of strain EB216 ($P > 0.05$), while the intracellular NADH level of strain EB216-ΔpykA decreased by 21% ($P < 0.05$) compared with that of strain EB216 (Table 6). This suggests an increased turnover rate of NADH in strain EB216-ΔpykA, which indicates that the NADH-consuming *n*-butanol pathway in EB216-ΔpykA strain is more active.

TABLE 6 Assay of intracellular concentrations of pyruvate, ATP, and NADH[a]

Strain	Intracellular level		
	Pyruvate (μmol/mg protein)	ATP (nmol/mg protein)	NADH (pmol/mg protein)
EB216	0.33 ± 0.04	3.37 ± 0.48	3,690 ± 355
EB216-ΔpykF	0.31 ± 0.02	2.33 ± 0.22	3,203 ± 277
EB216-ΔpykA	0.39 ± 0.01	8.43 ± 0.47	2,903 ± 193

[a]mg protein, milligrams of crude protein extract. The strains were grown in static 15-ml sealed BD tubes at 37°C. Three repeats were performed, and the error data represent standard deviations.

DISCUSSION

Previously, knockout of *pykA* was used to weaken pyruvate formation from PEP for enhancing production of PEP-derived metabolites. One example was the production of 3-deoxy-D-arabino-heptulosonic acid 7-phosphate (DAHP) from PEP. Knockout of *pykF* led to a 19%-improved DAHP titer, while knockout of *pykA* led to a 46%-improved DAHP titer, and double knockout of *pykA* and *pykF* led to a 235%-improved DAHP titer (31). Another example was the production of succinate from PEP. Knockout of *pykF* led to a 31%-improved succinate titer, while double knockout of *pykA* and *pykF* led to a 188%-improved succinate titer (32). In the present study, deletion of *pykA* was found to be associated with a significantly prolonged growth phase and with increased cell growth and production of pyruvate-derived *n*-butanol (Fig. 1A to C) under anaerobic conditions. This suggests that the role of PykA in glycolysis was overlooked and needs reexamination.

In the aerobic glycolysis pathway of *E. coli*, PykF is believed to be the major contributor of pyruvate kinase activity, while PykA contributes little (25, 26). Our enzymatic assay confirmed that PykA does contribute very little (7%) to total pyruvate kinase activity (Table 4). However, it is interesting that PykA contributes 30% of the total pyruvate kinase activity (Table 4) under anaerobic conditions. Previous studies also showed that the transcription of the *pykA* gene under anaerobic conditions could be improved up to 3-fold in comparison to that seen under aerobic conditions and that knockout of the *fnr* gene (encoding a fumarate and nitrate reductase [FNR] regulator which represses genes involved in aerobic respiration and activates genes required for anaerobic respiration) decreased the *pykA* transcription by 63% (33, 34). On the basis of those transcriptional analyses and our enzymatic analysis, we believe that *pykA* should not be considered a dispensable pyruvate kinase gene but plays an important role under anaerobic conditions in particular.

In association with its activity of converting PEP into pyruvate, PykA was also reported to have a broad specificity on nucleotide diphosphates, which could serve as acceptors of a energy-rich phosphate group from PEP and could take the place of nucleoside diphosphate kinase in supplying nucleoside triphosphates (27, 28). Determination of the specificity constant k_{cat}/K_m allowed us to systematically understand the differences in the levels of catalytic efficiency of PykA and PykF on four NDPs. PykA is mostly and equally active on ADP and UDP, followed by GDP and CDP. Waygood et al. (30) reported only the K_m of PykA on four NDPs (ADP, 0.08 mM; GDP, 0.13 mM; UDP, 0.25 mM; CDP, 0.39 mM). While the K_m value of PykA for ADP is consistent with our determination, the K_m values for the other three NDPs are quite different from our results. Interestingly, PykF was not active on GDP and CDP in our test, whereas the results documented in an earlier publication showed that PykF had a very high affinity to GDP (K_m, 0.05 mM) and very low affinity to CDP (K_m, 6.7 mM) (15). The K_m of PykF on ADP and UDP determined in our study is quite consistent with the literature, though (15). As the catalytic efficiency of PykA on GDP and CDP is comparable with the catalytic efficiency of PykF on ADP and UDP (Table 5), it is therefore conceivable that the phosphate group originally used for generation of GDP and CDP by PykA might be redirected for generation of ADP and UDP by PykF, when *pykA* is deleted. However, we should also note that the *in vitro* conditions used for determining the kinetic parameters of PykA and PykF were not the same as the conditions that are found inside the cells—a comprehensive quantitative understanding of why the intracellular ATP concentration in strain EB216-ΔpykA increased by 150% needs further investigation.

It is intriguing that our results (Fig. 1 and Table 3) showed that the deletion of *pykA* increased the rate of conversion from pyruvate to *n*-butanol but not the rate of conversion from glucose to pyruvate. However, the *n*-butanol pathway from pyruvate to *n*-butanol does not contain reactions requiring ATP; thus, the increased ATP level in *pykA* mutant cannot account for this phenomenon. We noticed the accumulation of pyruvate in strain EB216, suggesting that the rate of conversion of glucose to pyruvate surpassed the rate of conversion of pyruvate to *n*-butanol. In other words, the glycolysis

TABLE 7 Bacterial strains and plasmids used in this study

Strain or plasmid	Relevant characteristic(s)[a]	Reference or source
Strains		
E. coli BW25113	*lacI*^{q} *rrnB*$_{T14}$ Δ*lacZ*$_{WJ16}$ *hsdR514* Δ*araBAD*$_{AH33}$ Δ*rhaBAD*$_{LD78}$	16
E. coli BL21(DE3)	F$^-$ *ompT hsdSB* (r_B^- m_B^-) *gal dcm rne131* (DE3)	Laboratory storage
E. coli EB205	Derived from BW25113; Δ*yqhD*::*atoB* Δ*ldhA*::*hbd* Δ(*ackA-pta*)::*crt* Δ*adhE*::*ter* Δ*frdBC*::*adhE2* Δ*eutE*::*fdh*	This work
E. coli EB215	Derived from EB205; Δ(*hyc-hyp*)::FRT Δ*fdhF*::*fdh*	This work
E. coli EB216	Derived from EB215; Δ*mdh*::FRT	This work
E. coli EB216-Tn5-599#	Derived from EB216; *pykA* gene was inserted using a Tn*5* transposon	This work
E. coli EB216-ΔpykA	Derived from EB216; Δ*pykA*	This work
E. coli EB216-ΔpykF	Derived from EB216; Δ*pykF*	This work
E. coli EB216-ΔyhjX	Derived from EB216; Δ*yhjX*	This work
E. coli EB216-ΔpykA&pykF	Derived from EB216-ΔpykA; Δ*pykF*	This work
E. coli EB216-ΔpykA&yhjX	Derived from EB216-ΔpykA; Δ*yhjX*	This work
Plasmids		
pKmTsSacB	Skeleton plasmid for cloning, constructed from pK18mobsacB (ATCC) with thermosensitive *ori* of pKD46, *kan*	20
pKmTsSacB-yqhD::atoB	pKmTsSacB-based vector, containing *yqhD*up-*atoB*-*yqhD*down cassette, *kan*	This work
pKmTsSacB-ldhA::hbd	pKmTsSacB-based vector, containing *ldhA*up-*hbd*-*ldhA*down cassette, *kan*	This work
pKmTsSacB-(ackA-pta)::crt	pKmTsSacB-based vector, containing (*ackA-pta*)up-*crt*-(*ackA-pta*)down cassette, *kan*	This work
pKmTsSacB-adhE::ter	pKmTsSacB-based vector, containing *adhE*up-*ter*-*adhE*down cassette, *kan*	This work
pKmTsSacB-frdBC::adhE2	pKmTsSacB-based vector, containing *frdBC*up-*adhE2*-*frdBC*down cassette, *kan*	This work
pKmTsSacB-eutE::fdh	pKmTsSacB-based vector, containing *eutE*up-*fdh*-*eutE*down cassette, *kan*	This work
pKmTsSacB-fdhF::fdh	pKmTsSacB-based vector, containing *fdhF*up-*fdh*-*fdhF*down cassette, *kan*	This work
pKD4	*bla*, FRT, *kan*	16
pKD46	*bla*, *araC*, *gam-bet-exo*	16
pCP20	*bla*, *flp*, *cat*	16
pET30a	*kan*	Laboratory storage
pET30a-pykA	pET30a-based vector, containing His-tagged PykA gene, *kan*	This work
pET30a-pykF	pET30a-based vector, containing His-tagged PykF gene, *kan*	This work

[a]*bla*, ampicillin resistance gene; *kan*, kanamycin resistance gene; *gam-bet-exo*, Red recombinase genes; *flp*, flipase (Flp recombinase) gene; *cat*, chloramphenicol resistance gene; FRT, flipase recognition target.

rate in strain EB216 is higher than the rate seen with the introduced *n*-butanol pathway. Notably, pyruvate accumulation was slower and the peak value was lower in strain EB216-ΔpykA than in strain EB216. This suggests that with 30% decreased pyruvate kinase activity, the glycolysis rate in strain EB216-ΔpykA is reduced to a level that is more compatible with the rate seen with the introduced *n*-butanol pathway, leading to continuous carbon flux from glucose to *n*-butanol and resulting in improved *n*-butanol production. Moreover, activation of the *yhjX* gene in strain EB216-ΔpykA enabled reassimilation of pyruvate, which may also explain the slight improvement in the yield of *n*-butanol on glucose in strain EB216-ΔpykA.

In summary, the minimal pyruvate kinase activity of PykA seen under aerobic conditions led people to think PykA is not important for glycolysis. Although previous *in vivo* studies have shown PykA has a broad specificity on nucleotide diphosphates, no literature has correlated this feature with glycolysis ATP production. The retrieval of a PykA null mutant with stronger *n*-butanol-producing ability encouraged us to reexamine the role of PykA in glycolysis. It turned out that PykA accounts for 30% of the pyruvate kinase activity under anaerobic conditions, and PykA is presumably used for production of NTPs in the cells. Knocking out PykA can lead to an increase in ATP production while not obviously affecting glucose consumption and thus can be applied as a general strategy to improve production of pyruvate-derived metabolites.

MATERIALS AND METHODS

Bacterial strains, plasmids, and primers. *E. coli* BW25113 (16) was used for construction of *n*-butanol-producing strains as the wild type. All primers were synthesized by Invitrogen (Beijing, China) followed by polyacrylamide gel electrophoresis purification. All strains and plasmids used in this study are listed in Table 7. Primers are listed in Table S2 in the supplemental material.

Construction of plasmids for gene integration. Plasmid pKmTsSacB (20) was used as a skeleton plasmid for constructing various recombinant plasmids. A constitutive tac promoter (miniPtac) (20, 35) which was introduced into the forward primer, was used for gene expression. Recombinant plasmid pKmTsSacB-yqhD::atoB was constructed for integration of the *atoB* gene into the genome of *E. coli* BW25113 at its *yqhD* site (Δ*yqhD*::*atoB*). First, the *atoB* gene was amplified from the genomic DNA of BW25113 using primers yqhD::atoB-3, yqhD::atoB, and yqhD::atoB-4. Second, the *yqhD* upstream and downstream fragments were amplified from genomic DNA of BW25113 using primer pairs yqhD::atoB-1/yqhD::atoB-2 and yqhD::atoB-5/yqhD::atoB-6, respectively. Third, the amplified *atoB* gene and the two fragments described above were spliced through BamHI and XbaI sites to form the "*yqhD*up-*atoB*-*yqhD*down" cassette *in vitro*. Finally, this *yqhD*up-*atoB*-*yqhD*down cassette was inserted into the XhoI and PstI sites of plasmid pKmTsSacB to generate plasmid pKmTsSacB-yqhD::atoB. In a similar manner, plasmids pKmTsSacB-ldhA::hbd (Δ*ldhA*::*hbd* [*hbd* from *Clostridium acetobutylicum*]), pKmTsSacB-ackA-pta::crt [Δ(*ackA-pta*)::*crt* (*crt* from *C. acetobutylicum*)], pKmTsSacB-adhE::ter (Δ*adhE*::*ter* [*ter* from *Treponema denticola*]), pKmTsSacB-frdBC::adhE2 (Δ*frdBC*::*adhE2* [*adhE2* from *C. acetobutylicum*]), and pKmTsSacB-eutE::fdh (Δ*eutE*::*fdh* [*fdh* from *Candida boidinii*]) were constructed using their respective primers (listed in Table S2). PCR enzymes, restriction enzymes, and T4 DNA ligase were purchased from New England BioLabs (Beijing, China).

Strain development. Six genes involved in production of *n*-butanol were integrated into the BW25113 chromosome at their respective chosen sites, one after another. Briefly, the pKmTsSacB-based recombinant plasmid was transformed into *E. coli* BW25113 by the use of a Gene Pulser system (Bio-Rad Laboratories, Inc., Richmond, CA) and plated on agar with kanamycin. Positive single-crossover integrants were separately streaked on agar plates supplemented with sucrose to screen for double-crossover integration. The correct integrant, verified by colony PCR and DNA sequencing, was selected for integrating the next gene (20). Finally, a strain with six *n*-butanol pathway genes (*atoB*, *hbd*, *crt*, *ter*, *adhE2*, and *fdh*, respectively) integrated at the *yqhD*, *ldhA*, *ackA-pta*, *adhE*, *frdBC*, and *eutE* sites was obtained and designated EB205. Subsequently, the *hyc* operon and *hyp* operon of strain EB205 were deleted following Red recombinase-based one-step inactivation of chromosomal genes (16), followed by integrating a modified *fdh* gene from *C. boidinii* which was codon optimized for *E. coli* into the *fdhF* site under the control of the native *fdhF* promoter, resulting in strain EB215. Furthermore, the NADH consumption *mdh* gene of strain EB215 was deleted to generate strain EB216. A Red-mediated recombination method (16) was used for further deletion of *pykA*, *pykF*, and *yhjX* genes. All strains developed in this study were listed in Table 7.

Tn*5* transposon-based screening for new targets. The genome-wide random mutagenesis of strain EB216 was carried out using a EZ-Tn*5* <KAN-2> TNP Transposome kit (Epicentre, Madison, WI), following the manufacturer's instructions. In a previous experiment (data not shown), it was noticed that a high titer of *n*-butanol was always associated with a low extracellular concentration of pyruvate and high optical density (OD). Therefore, mutants were screened by measuring the OD at 600 nm (OD_{600}) of the bacterial cells, the pyruvate concentration in the screening broth, and the ratio of the pyruvate concentration to the OD_{600} of each mutant. The mutant colonies were inoculated into deep 96-well plates (containing 1.25 ml fermentation medium per well) by the use of a QPIX2 robotic colony picker (Molecular Devices Co.) and were incubated in a Shellab Bactron I-2 anaerobic chamber (Sheldon Manufacturing Inc.) filled with an anaerobic gas mixture (5% CO_2, 5% H_2, and 90% N_2) for 3 days. For optical density measurements, 200 μl of culture was transferred to a standard 96-well plate and the OD_{600} was determined. For pyruvate concentration measurements, 80 μl of 25-fold-diluted culture, 80 μl of 0.0375% 2,4-dinitrophenylhydrazine (DNPH), and 80 μl of 2.81 mol/liter NaOH were mixed and the absorbance at 520 nm was determined after a 10-min reaction (36). All measurements were performed by using a Biomek 3000 laboratory automation workstation (Beckman Coulter Inc.). A Tecan Infinite M200 plate reader (Tecan Austria GmbH, Grödig, Austria) was used for absorbance detection. Mutants with a low ratio of pyruvate concentration/OD_{600} were selected for the second-round screening.

The second-round screening was carried out using HPLC analysis of *n*-butanol after tube fermentation. The best *n*-butanol-producing mutants were collected to extract genomic DNA using an E.Z.N.A. bacterial DNA isolation kit (Omega Biotek Inc.) for the NGS, which was completed and analyzed by Genewiz, Inc. (Genewiz, Suzhou, China).

Growth and maintenance conditions. *E. coli* strains were grown aerobically at 30°C or 37°C in Luria-Bertani (LB) medium (10 g/liter tryptone, 5 g/liter yeast extract, 10 g/liter NaCl) supplemented, when necessary, with ampicillin (100 μg/ml), chloramphenicol (30 μg/ml), or kanamycin (50 μg/ml). Strains were maintained frozen in 15% glycerol at −80°C. Before culturing, fresh colonies were picked from LB plates and inoculated into LB medium at 37°C and 200 rpm for 12 h. Unless otherwise indicated, 5% of this culture was inoculated into the fresh medium. For batch culture, M9 mineral salt (17.1 g $Na_2HPO_4 \cdot 12H_2O$, 3 g KH_2PO_4, 0.5 g NaCl, 1 g NH_4Cl, 2 mmol $MgSO_4$, and 0.1 mmol $CaCl_2$ per liter water) supplemented with 2 g/liter yeast extract (M9Y) (37) and 20 g/liter glucose was used. Tube fermentation was performed in 10 ml medium in a sealed 15-ml polypropylene conical tube (BD Biosciences, San Jose, CA) in a 37°C incubator without shaking for 48 h or longer when necessary. Bioreactor fermentation was carried out in a 7.5-liter BioFlo 110 bioreactor with 4 liters of medium (New Brunswick Scientific, Edison, NJ) for 72 h. Cells were grown at 37°C and 200 rpm without pH control.

Transcriptome sequencing. Cell cultures growing in a fermenter for 6 h, 12 h, 24 h, and 48 h were harvested by centrifugation and frozen at −80°C. RNA isolation, construction of cDNA libraries, and sequencing were performed by Genewiz, Inc. (Genewiz, Suzhou, China). Briefly, total RNAs were isolated using TRIzol (38, 39). For construction of cDNA libraries, an Illumina TruSeq RNA Sample Prep kit (Illumina,

San Diego, CA) was used. After purification, detection, and quantification, the libraries were sequenced by the use of a HiSeq 2000 system (Illumina, San Diego, CA).

Transcriptomic analysis. Transcriptomic analysis was also carried out by Genewiz, Inc. Raw data in FASTQ format were processed by Trimmomatic (v0.30) (40) to obtain the clean data, which were then evaluated using FastQC (v0.10.1; http://www.bioinformatics.babraham.ac.uk/projects/fastqc/). The average quality score exceeded 30, which indicated good sequencing quality. Subsequently, clean data reads were mapped onto the *E. coli* BW25113 genome (GenBank accession number CP009273.1) using Bowtie2 (41). Quantification of gene expression and analysis of gene differential expression were performed using FPKM-based RSEM software (v1.2.4) (42) and edgeR (v3.4.2) (Bioconductor), respectively. Differentially expressed genes that showed more than a 2-fold change and a lower false-discovery rate (FDR) ($\leq$0.05) were defined as the significantly differentially expressed genes.

Analytical procedure. Cell density in the tube or fermenter was determined by the use of a UV-visible light spectrophotometer (UV-2802PC; Unico, Shanghai, China) with the optical density at 600 nm (OD_{600}). The sugar, organic acid, and alcohol concentrations of fermentation samples were analyzed by the use of an Agilent 1260 HPLC system (Agilent Technologies, Santa Clara, CA). A Bio-Rad HPX-87H column (Bio-Rad Laboratories, Inc., Richmond, CA) was used with 5 mM H_2SO_4 as the mobile phase (10 μl injection, 0.5 ml/min, 15°C) for HPLC analysis.

Cells growing at the mid-exponential-growth phase were harvested to prepare the crude extract by sonication (Hongdaxinchen Biotechnology Co., Ltd., Beijing, China) for enzyme and intracellular metabolite assays. Specifically, the pyruvate kinase assay was implemented based on previous studies (15, 43, 44). The activities of PykF and PykA were detected with the addition of their respective activators FBP and AMP. A 1 mM concentration of FBP could bring PykF to 80% of its maximal velocity without affecting the activity of PykA, while 1 mM AMP would bring PykA to its maximal velocity without affecting the activity of PykF (44). A classic lactate dehydrogenase-coupled reaction was used to detect the decrease in absorbance of NADH at 340 nm using a microtiter plate reader. The standard assay mixture contains the following components (in a final volume of 200 μl): 30 mmol/liter HEPES (pH 7.5); 10 mmol/liter $MgCl_2$; 10 mmol/liter KCl; 2 mmol/liter ADP; 1 mmol/liter PEP; 0.15 mmol/liter NADH; 20 units of bacterial lactate dehydrogenase; and 1 mmol/liter FBP or 1 mmol/liter AMP for the activation of PykF or PykA. The reaction was started by the addition of the crude extract and was carried out at 25°C. A molar extinction coefficient for NADH of 6.22×10^3 liters/mol · cm was used for converting changes in absorbance into moles of pyruvate formed per minute.

To further determine the kinetic parameters of the two pyruvate kinases, UDP, GDP, and CDP were used as substitutes for ADP. Pyruvate kinases expressed on pET30a vector in *E. coli* BL21(DE3) were purified using immobilized metal affinity chromatography (IMAC) (45). The intracellular concentrations of pyruvate, ATP, and NADH were immediately determined after sampling using a pyruvate assay kit (BioAssay Systems, Hayward, CA), an ATP fluorometric assay kit (BioVision Incorporated, Milpitas, CA), and an NADH fluorometric assay kit (BioVision Incorporated, Milpitas, CA) according to the manufacturers' instructions, respectively. Measurement was performed after sampling and disrupting the cells by sonication at 140 W for 1 min on ice (46, 47). The protein concentration in the cell extracts was quantified by using a Coomassie brilliant blue protein assay kit (Comin Biotechnology Co., Ltd., Suzhou, China). A Tecan Infinite M200 plate reader was used to detect absorbance at different wavelengths. All the reagents mentioned were purchased from Sigma (Sigma-Aldrich Co., Shanghai, China) or Yuanye (Yuanye Biotek, Shanghai, China).

Statistical analysis. The statistical analysis of data and plots was performed using Student's *t* test in SPSS software when necessary. *P* values of $<$0.05 were considered to indicate statistical significance.

Accession number(s). High-throughput sequence data (RNA-seq) from strain EB216 and strain EB216-ΔpykA at different fermentation time points have been deposited into the NCBI GEO database under accession number GSE96551.

SUPPLEMENTAL MATERIAL

Supplemental material for this article may be found at https://doi.org/10.1128/AEM.00316-17.

SUPPLEMENTAL FILE 1, PDF file, 0.1 MB.

ACKNOWLEDGMENTS

We are grateful to Huawei Zhu from our laboratory and Simi Jasmin Zhang (University of Waterloo, Waterloo, Ontario, Canada) for critical reading of the manuscript. We thank Hongwei Yu and Huailin Zhou (Institute of Botany, CAS, Beijing, China) for their help with statistical analysis. We also thank Guoxia Liu from our laboratory for the kind help of enzyme kinetic data analysis.

This study was funded by the National Natural Science Foundation of China (grant number 31270107), the National High Technology Research and Development Program of China (grant number 2011AA02A208), and the CAS/SAFEA International Partnership Program for Creative Research Teams.

REFERENCES

1. Jeffries TW. 2005. Ethanol fermentation on the move. Nat Biotechnol 23:40–41. https://doi.org/10.1038/nbt0105-40.
2. Shen CR, Lan EI, Dekishima Y, Baez A, Cho KM, Liao JC. 2011. Driving forces enable high-titer anaerobic 1-butanol synthesis in *Escherichia coli*. Appl Environ Microbiol 77:2905–2915. https://doi.org/10.1128/AEM.03034-10.
3. Yim H, Haselbeck R, Niu W, Pujol-Baxley C, Burgard A, Boldt J, Khandurina J, Trawick JD, Osterhout RE, Stephen R, Estadilla J, Teisan S, Schreyer HB, Andrae S, Yang TH, Lee SY, Burk MJ, Van Dien S. 2011. Metabolic engineering of *Escherichia coli* for direct production of 1,4-butanediol. Nat Chem Biol 7:445–452. https://doi.org/10.1038/nchembio.580.
4. Lee JW, Kim HU, Choi S, Yi J, Lee SY. 2011. Microbial production of building block chemicals and polymers. Curr Opin Biotechnol 22:758–767. https://doi.org/10.1016/j.copbio.2011.02.011.
5. Peralta-Yahya PP, Zhang F, del Cardayre SB, Keasling JD. 2012. Microbial engineering for the production of advanced biofuels. Nature 488:320–328. https://doi.org/10.1038/nature11478.
6. Koebmann BJ, Westerhoff HV, Snoep JL, Dan N, Jensen PR. 2002. The glycolytic flux in *Escherichia coli* is controlled by the demand for ATP. J Bacteriol 184:3909–3916. https://doi.org/10.1128/JB.184.14.3909-3916.2002.
7. Xue C, Zhao J, Lu C, Yang S-T, Bai F, Tang I-C. 2012. High-titer *n*-butanol production by *Clostridium acetobutylicum* JB200 in fed-batch fermentation with intermittent gas stripping. Biotechnol Bioeng 109:2746–2756. https://doi.org/10.1002/bit.24563.
8. Atkinson DE. 1968. Energy charge of the adenylate pool as a regulatory parameter. Interaction with feedback modifiers. Biochemistry 7:4030–4034.
9. Shen L, Fall L, Walton GM, Atkinson DE. 1968. Interaction between energy charge and metabolite modulation in the regulation of enzymes of amphibolic sequences. Phosphofructokinase and pyruvate dehydrogenase. Biochemistry 7:4041–4045.
10. Shen LC, Atkinson DE. 1970. Regulation of pyruvate dehydrogenase from *Escherichia coli* interactions of adenylate energy charge and other regulatory parameters. J Biol Chem 245:5974–5978.
11. Kim D-M, Swartz JR. 2000. Oxalate improves protein synthesis by enhancing ATP supply in a cell-free system derived from *Escherichia coli*. Biotechnol Lett 22:1537–1542. https://doi.org/10.1023/A:1005624811710.
12. Singh A, Soh KC, Hatzimanikatis V, Gill RT. 2011. Manipulating redox and ATP balancing for improved production of succinate in *E. coli*. Metab Eng 13:76–81. https://doi.org/10.1016/j.ymben.2010.10.006.
13. Kraaijenhagen RJ, van der Heijden MCM, Streefkerk M, Rijksen G, de Gast GC, Staal GEJ. 1984. Hexokinase, phosphofructokinase and pyruvate kinase isozymes in lymphocyte subpopulations. Clin Chim Acta 140:65–76. https://doi.org/10.1016/0009-8981(84)90152-9.
14. Flores N, Xiao J, Berry A, Bolívar F, Valle F. 1996. Pathway engineering for the production of aromatic compounds in *Escherichia coli*. Nat Biotechnol 14:620–623. https://doi.org/10.1038/nbt0596-620.
15. Waygood EB, Sanwal B. 1974. The control of pyruvate kinases of *Escherichia coli*. I. Physicochemical and regulatory properties of the enzyme activated by fructose 1,6-diphosphate. J Biol Chem 249:265–274.
16. Datsenko KA, Wanner BL. 2000. One-step inactivation of chromosomal genes in *Escherichia coli* K-12 using PCR products. Proc Natl Acad Sci U S A 97:6640–6645. https://doi.org/10.1073/pnas.120163297.
17. Lin Z, Dong H, Li Y. 2015. Improvement of butanol production by *Escherichia coli* using Tn5 transposon. Sheng Wu Gong Cheng Xue Bao 31:1711–1719. (In Chinese.)
18. Ponce E, Martínez A, Bolívar F, Valle F. 1998. Stimulation of glucose catabolism through the pentose pathway by the absence of the two pyruvate kinase isoenzymes in *Escherichia coli*. Biotechnol Bioeng 58:292–295. https://doi.org/10.1002/(SICI)1097-0290(19980420)58:2/3<292::AID-BIT25>3.0.CO;2-D.
19. Dong H, Zhang Y, Dai Z, Li Y. 2010. Engineering *Clostridium* strain to accept unmethylated DNA. PLoS One 5:e9038. https://doi.org/10.1371/journal.pone.0009038.
20. Sun L, Yang F, Sun H, Zhu T, Li X, Li Y, Xu Z, Zhang Y. 2016. Synthetic pathway optimization for improved 1,2,4-butanetriol production. J Ind Microbiol Biotechnol 43:67–78. https://doi.org/10.1007/s10295-015-1693-7.
21. Marisch K, Bayer K, Cserjan-Puschmann M, Luchner M, Striedner G. 2013. Evaluation of three industrial *Escherichia coli* strains in fed-batch cultivations during high-level SOD protein production. Microb Cell Fact 12:58. https://doi.org/10.1186/1475-2859-12-58.
22. Fried L, Behr S, Jung K. 2013. Identification of a target gene and activating stimulus for the YpdA/YpdB histidine kinase/response regulator system in *Escherichia coli*. J Bacteriol 195:807–815. https://doi.org/10.1128/JB.02051-12.
23. Lang VJ, Leystra-Lantz C, Cook RA. 1987. Characterization of the specific pyruvate transport system in *Escherichia coli* K-12. J Bacteriol 169:380–385. https://doi.org/10.1128/jb.169.1.380-385.1987.
24. Kannan G, Wilks JC, Fitzgerald DM, Jones BD, Bondurant SS, Slonczewski JL. 2008. Rapid acid treatment of *Escherichia coli*: transcriptomic response and recovery. BMC Microbiol 8:37. https://doi.org/10.1186/1471-2180-8-37.
25. Ponce E, Flores N, Martínez A, Valle F, Bolívar F. 1995. Cloning of the two pyruvate kinase isoenzyme structural genes from *Escherichia coli*: the relative roles of these enzymes in pyruvate biosynthesis. J Bacteriol 177:5719–5722. https://doi.org/10.1128/jb.177.19.5719-5722.1995.
26. Meza E, Becker J, Bolívar F, Gosset G, Wittmann C. 2012. Consequences of phosphoenolpyruvate: sugar phosphotranferase [sp.] system and pyruvate kinase isozymes inactivation in central carbon metabolism flux distribution in *Escherichia coli*. Microb Cell Fact 11:127. https://doi.org/10.1186/1475-2859-11-1.
27. Saeki T, Hori M, Umezawa H. 1974. Pyruvate kinase of *Escherichia coli*. J Biochem 76:631–637. https://doi.org/10.1093/oxfordjournals.jbchem.a130607.
28. Lu Q, Zhang X, Almaula N, Mathews CK, Inouye M. 1995. The gene for nucleoside diphosphate kinase functions as a mutator gene in *Escherichia coli*. J Mol Biol 254:337–341. https://doi.org/10.1006/jmbi.1995.0620.
29. McCloskey D, Gangoiti JA, King ZA, Naviaux RK, Barshop BA, Palsson BO, Feist AM. 2014. A model-driven quantitative metabolomics analysis of aerobic and anaerobic metabolism in *E. coli* K-12 MG1655 that is biochemically and thermodynamically consistent. Biotechnol Bioeng 111:803–815. https://doi.org/10.1002/bit.25133.
30. Waygood EB, Rayman MK, Sanwal B. 1975. The control of pyruvate kinases of *Escherichia coli* II. Effectors and regulatory properties of the enzyme activated by ribose 5-phosphate. Can J Biochem 53:444–454.
31. Gosset G, Yong-Xiao J, Berry A. 1996. A direct comparison of approaches for increasing carbon flow to aromatic biosynthesis in *Escherichia coli*. J Ind Microbiol 17:47–52. https://doi.org/10.1007/BF01570148.
32. Lee SJ, Lee DY, Kim TY, Kim BH, Lee J, Lee SY. 2005. Metabolic engineering of *Escherichia coli* for enhanced production of succinic acid, based on genome comparison and in silico gene knockout simulation. Appl Environ Microbiol 71:7880–7887. https://doi.org/10.1128/AEM.71.12.7880-7887.2005.
33. Covert MW, Knight EM, Reed JL, Herrgard MJ, Palsson BO. 2004. Integrating high-throughput and computational data elucidates bacterial networks. Nature 429:92–96. https://doi.org/10.1038/nature02456.
34. Shalel-Levanon S, San KY, Bennett GN. 2005. Effect of ArcA and FNR on the expression of genes related to the oxygen regulation and the glycolysis pathway in *Escherichia coli* under microaerobic growth conditions. Biotechnol Bioeng 92:147–159. https://doi.org/10.1002/bit.20583.
35. de Boer HA, Comstock LJ, Vasser M. 1983. The tac promoter: a functional hybrid derived from the trp and lac promoters. Proc Natl Acad Sci U S A 80:21–25. https://doi.org/10.1073/pnas.80.1.21.
36. Eze LC, Echetebu CO. 1980. Some properties of aspartate and alanine aminotransferases from *Trichoderma viride*. J Gen Microbiol 120:523–527.
37. Saini M, Hong Chen M, Chiang CJ, Chao YP. 2015. Potential production platform of *n*-butanol in *Escherichia coli*. Metab Eng 27:76–82. https://doi.org/10.1016/j.ymben.2014.11.001.
38. Simms D, Cizdziel PE, Chomczynski P. 1993. TRIzol: a new reagent for optimal single-step isolation of RNA. Focus 15:532–535.
39. Rio DC, Ares M, Hannon GJ, Nilsen TW. 2010. Purification of RNA using TRIzol (TRI reagent). Cold Spring Harb Protoc 2010:pdb.prot5439. https://doi.org/10.1101/pdb.prot5439.
40. Lohse M, Bolger A, Nagel A, Fernie AR, Lunn JE, Stitt M, Usadel B. 2012. RobiNA: a user-friendly, integrated software solution for RNA-Seq-based transcriptomics. Nucleic Acids Res 40:W622–W627. https://doi.org/10.1093/nar/gks540.
41. Langmead B, Salzberg SL. 2012. Fast gapped-read alignment with Bowtie 2. Nat Methods 9:357–359. https://doi.org/10.1038/nmeth.1923.
42. Li B, Dewey CN. 2011. RSEM: accurate transcript quantification from

RNA-Seq data with or without a reference genome. BMC Bioinformatics 12:323. https://doi.org/10.1186/1471-2105-12-323.
43. Kotlarz D, Garreau H, Buc H. 1975. Regulation of the amount and of the activity of phosphofructokinases and pyruvate kinases in *Escherichia coli*. Biochim Biophys Acta 381:257–268. https://doi.org/10.1016/0304-4165(75)90232-9.
44. Malcovati M, Valentini G. 1982. AMP- and fructose 1,6-bisphosphate-activated pyruvate kinases from *Escherichia coli*. Methods Enzymol 90:170–179. https://doi.org/10.1016/S0076-6879(82)90123-9.
45. Bornhorst JA, Falke JJ. 2000. Purification of proteins using polyhistidine affinity tags. Methods Enzymol 326:245–254. https://doi.org/10.1016/S0076-6879(00)26058-8.
46. Kim H-J, Kwon YD, Lee SY, Kim P. 2012. An engineered *Escherichia coli* having a high intracellular level of ATP and enhanced recombinant protein production. Appl Microbiol Biotechnol 94:1079–1086. https://doi.org/10.1007/s00253-011-3779-0.
47. Na Y-A, Lee J-Y, Bang W-J, Lee HJ, Choi S-I, Kwon S-K, Jung K-H, Kim JF, Kim P. 2015. Growth retardation of *Escherichia coli* by artificial increase of intracellular ATP. J Ind Microbiol Biotechnol 42:915–924. https://doi.org/10.1007/s10295-015-1609-6.